On the stability of the troposphere/lower stratosphere and its relationships with cirrus clouds and three mandatory levels over Buenos Aires

Adrián E. Yuchechen, S. Gabriela Lakkis & Mario B. Lavorato

Published online: 02 Mar 2016.

Submit your article to this journal ↗

View related articles ↗

View Crossmark data ↗

Taylor & Francis
Taylor & Francis Group

On the stability of the troposphere/lower stratosphere and its relationships with cirrus clouds and three mandatory levels over Buenos Aires

Adrián E. Yuchechen [a,b,c], S. Gabriela Lakkis[b,d] and Mario B. Lavorato[e]

aConsejo Nacional de Investigaciones Científicas y Técnicas (CONICET), Buenos Aires, Argentina; bUnidad de Investigación y Desarrollo de las Ingenierías (UIDI), Facultad Regional Buenos Aires (FRBA), Universidad Tecnológica Nacional (UTN), Buenos Aires, Argentina; cFacultad de Ciencias Fisicomatemáticas e Ingeniería, Universidad Católica Argentina (UCA), Buenos Aires, Argentina; dFacultad de Ciencias Agrarias, UCA, Buenos Aires, Argentina; eDivisión Radar Láser, Instituto de Investigaciones Científicas y Técnicas para la Defensa (CITEDEF), Villa Martelli, Argentina

ABSTRACT

An unrotated principal components analysis was carried out to establish the most representative modes for the joint variability between the heights of the upper and lower boundaries of cirrus clouds and three different mandatory levels (850, 500, and 100 hPa), and the associated stability of the troposphere over Buenos Aires. Discussion is limited to the first three most representative structures found, which consists of spatial patterns (or empirical orthogonal functions, EOFs) and their time-evolving coefficients (or principal components, PCs). EOF_1 shows a direct (indirect) mode that encompasses the cirrus slightly below (above) its mean position, with 500 and 100 hPa exhibiting a similar behaviour and 850 hPa acting the opposite way. EOF_1 is associated with above-normal stability (instability) for direct (indirect) modes (i.e. positive (negative) values of PC_1). On a monthly average, this occurs in the austral winter (summer) months. Regarding EOF_2, all three mandatory levels experience positive (negative) height anomalies in direct (indirect) modes and cirrus goes up (down) under mild stability (instability). Monthly averages show that PC_2 is approximately positive in summer and in early fall and negative the rest of the year. As to EOF_3, it is characterized by a stability similar to that of EOF_2, with direct (indirect) modes showing lowered (raised) cirrus and all three mandatory levels above (below) normal conditions; on a monthly basis, PC_3 is best described as having a semi-annual evolution, with maxima (minima) in March and October (January and August). Overall, EOF_1 has the highest stability or instability, depending upon the sign of PC_1. These results are the first of their kind worldwide.

1. Introduction

Clouds have been classified since the 19th century using the terminology coined by Howard (1865). This classification is based on their shape and appearance as seen from

---

CONTACT Adrián E. Yuchechen ✉ aeyuchechen@frba.utn.edu.ar 🏢 Unidad de Investigación y Desarrollo de las Ingenierías (UIDI), Facultad Regional Buenos Aires (FRBA), Universidad Tecnológica Nacional (UTN), Mozart 2300, C1407IVT, Ciudad Autónoma de Buenos Aires, Argentina.

the ground. Within that classification, cirrus clouds can be described as thin and often wispy clouds, typically found at high heights and composed of ice crystals that originate from the freezing of supercooled haze particles (Sassen 2002). The impact of cirrus clouds on the Earth's climate strongly depend on their physical properties, the most relevant of these being the altitude, distance to the tropopause, mid-cloud temperature, thermal contrast with the surface, geometrical and optical depth (OD), and extinction coefficient. With the purpose of obtaining realistic ranges of values for these properties, numerous analyses have been carried out at different latitude bands after the pioneer research efforts on ice crystal clouds made by Ludlam (1951) and London (1957). Over Buenos Aires (34.6° S, 58.5° W), cirrus clouds were analysed in Lakkis, Lavorato, and Canziani (2009) and Lakkis et al. (2015). Following the criteria adopted by Sassen and Cho (1992), cirrus were found to be optically thin ($0.03 < OD < 0.3$), and usually located at 8–11 km with mid-cloud temperatures varying between −75 and −55ºC. Clouds whose base altitudes display significant variability while their tops remain close to the tropopause show geometrical thicknesses ranging from 1.2 to 5 km.

The role these clouds play in the atmosphere is mainly related to the radiative budget (Wylie et al. 1994), but their formation mechanisms, presence, and persistence are associated with weather processes' instability phenomena and convective processes. Fujita (1982) described the role of cirrus in the dynamically driven mechanism occurring above severe thunderstorms as 'jumping cirrus'. Wang (2004) showed in his analysis of a storm observed in southeastern Montana that the behaviour of Fujita's jumping cirrus can be explained by gravity-wave-breaking mechanisms atop thunderstorms. Gravity-wave phenomena are often present within cirrus cloud systems and may influence, or be influenced by, cirrus cloud processes (Stephens 2002). Such waves are excited by the strong updrafts in the storm, and the breaking is caused by high instability near the cloud top.

A comparison between two different radar readings permitted Wada et al. (2005) to observe the formation of cirrus clouds as a result of turbulence mixing created by shear instabilities in a frontal zone over Japan. They proposed that Kelvin–Helmholtz instability (KHI), strongly related to turbulence, is responsible for the formation of such cirrus clouds through mixing of two different air masses. In Japan, Luce et al. (2012) analysed the presence of small-scale perturbations of temperature and humidity fields off a frontal zone, and suggested that KHI may have been the consequence of the presence of cirrus clouds that had been advected by a jet stream away from convective clouds belonging to a deep low-pressure system. In the tropical upper troposphere and lower stratosphere, cirrus clouds are linked to deep convection, since the clouds themselves are a sink for water vapour through the growth and fallout of ice particles (Sassen, Wang, and Liu 2009, and references therein).

Cirrus clouds have been linked with stratosphere–troposphere exchange events, which are usually related to tropopause-level jet streams, overshooting deep convective systems, and tropopause folds connected to extra-tropical cyclones, where an enhanced exchange between the stratosphere and the troposphere can be observed. Results indicate that cirrus clouds alter the tropopause region by changing the potential stability close to it, reducing humidity and convectively mixing lower air up to higher regions (Reutter and Spichtinger 2013). Given the proximity of cirrus clouds to the tropopause, they are thought to play a key role in the dehydration of the stratosphere

through 'freeze-drying' air to the saturation vapour pressure at the cold-point tropopause temperature as it slowly ascends through the tropical tropopause layer (Jensen et al. 2008, and references therein).

In summary, cirrus clouds and instability processes are well connected and many efforts have been devoted to investigating the presence of these clouds, their formation mechanisms, and their lifetime and persistence, related to instability processes in the atmosphere. Atmospheric instability can be addressed by means of instability indices, which provide a real-time overview of atmospheric conditions. The World Meteorological Organization (WMO) defines a mandatory level as a 'standard pressure level for which temperature and wind data obtained from upper-air soundings must be reported' (WMO 1992). To the best of our knowledge, research efforts that link cirrus clouds to both instability indices and mandatory levels do not exist in the literature. The work here is motivated by the lack of such studies. It is aimed at establishing the most representative patterns for the joint variability between the thickness of cirrus clouds, the geopotential height of 850, 500, and 100 hPa, and five instability indices over Buenos Aires.

2. Data and methodology

Geopotential height data for both the bottom and top of cirrus clouds were calculated from lidar measurements spanning the period 2002–2007. They were taken at different times at the Instituto de Investigaciones Científicas y Técnicas para la Defensa (CITEDEF), located in Villa Martelli, Buenos Aires Metropolitan Area. Both the procedure and the technical specifications of the equipment used for these measurements can be found in Lakkis, Lavorato, and Canziani (2009). The original data set consisted of 174 different observations but not all of them are used, as will be explained below. Corresponding geopotential height data for 850, 500, and 100 hPa and the instability index time series, spanning the period 1973–2013, were extracted from radiosonde ascents launched at Ezeiza Airport (SAEZ, 34.81° S, 58.53° W), approximately 25 km southwest of the lidar station. These ascents are in the public domain at the University of Wyoming worldwide radiosonde database, which includes comprehensive information dating from 1973 and is available at http://weather.uwyo.edu. Each ascent includes a number of parameters (e.g. geopotential height and temperature) for both mandatory (i.e. fixed pressure) and significant levels, and also includes the calculated values for different derived indices that characterize the atmospheric state.

The instability indices used here are the Showalter index (SI), the Lifted index (LI), the total totals index (TT), the SWEAT Index (SW), and the K-index (KI). A brief description of each of them is given towards interpretation of the results. The first index is defined by $SI = T'_{500} - T_{500}$, where T'_{500} denotes the environmental temperature at 500 hPa and T_{500} denotes the temperature a parcel would attain at 500 hPa if it were lifted from 850 hPa. LI is defined in a similar fashion, but the parcel is raised from the surface (or near it). In any case, only temperature and dewpoint at the level from which the parcel is raised and the temperature at 500 hPa are required in order to calculate both indices. Both can be either positive or negative. Broadly speaking, the more negative (or less positive) they become, the greater the potential for instability in the atmosphere (Petty 2008, 267–275).

Intermediate indices, the vertical totals index (VT) and the cross-totals index (CT), are defined, as follows, in order to build an expression for TT: $VT = T_{850} - T_{500}$ and $CT = T_{d,850} - T_{500}$, where T_{850} and $T_{d,850}$ denote temperature and dewpoint at 850 hPa, respectively. TT was first defined as the addition of VT and CT (as quoted in Miller 1972). TT has the advantage, unlike SI and LI, that it considers low-level moisture, although the use of TT is unhelpful when most of the moisture lies below the 850 hPa level. SW was first introduced by Miller in 1967 (as quoted in Miller 1972) and takes into account thermal instability (through TT), low-level moisture, horizontal wind, and vertical wind shear. Its expression is $SW = 12T_{d,850} + 20(TT - 49) + 2f_{850} + f_{500} + 125(s + 0.2)$, where f_{850} and f_{500} represent the wind speed (in knots) at 850 and 500 hPa, respectively, and s denotes the sine between the wind direction at 500 and 850 hPa to account for the advection of warm air. All the terms in the expression should be strictly positive and are set to zero otherwise. KI is similar to TT, but also accounts for temperature and moisture at 700 hPa. It is defined as $KI = T_{850} - T_{500} + T_{d,850} - (T_{700} - T_{d,700})$. For TT, SW, and KI, instability is greater when their values are more positive.

The inclusion of geopotential height for the top and the bottom of the cirrus clouds is not only crucial to calculating their thickness, but also to fulfil one of the goals of the paper (i.e. the links with instability). Geopotential height data for the 850 and 500 hPa levels have been included in the analysis because the former (latter) represents the lower (middle) troposphere. Furthermore, thermodynamic and dynamic variables for these two levels are used to build most of the aforementioned indices, but the geopotential height is not. Additionally, we wanted to use a variable that was directly comparable to that defining the top and bottom of the cirrus clouds. Regarding the inclusion of 100 hPa, the level has been traditionally used as a proxy for the tropical tropopause, whereas at mid- and high latitudes it constitutes the uppermost level of the so-called 'lowermost stratosphere.' (Holton et al. 1995).

There are different launch times in the radiosonde database at SAEZ within the period it spans. However, only radiosondes launched at 12Z (i.e. noon at Greenwich) are available for the period covered by the lidar measurements. A simple selection procedure was applied to radiosonde data in order to identify potentially erroneous values. For the period 1973–2013, the climatological monthly mean and standard deviation were calculated at the three mandatory levels, as well as for the five instability indices. Data were not included in the analysis if the anomaly with respect to the corresponding monthly mean exceeded two units of standard deviation for that month. The rest of the information was used to fill in a matrix having 10 rows, one for each study variable, two of them being the upper and lower limits of the cirrus clouds, and 174 columns, each one representing a different cirrus measurement.

Owing to missing radiosonde data, the number of cirrus observations studied here was 128. Figure 1 shows the distribution of such observations broken down in a monthly fashion. Missing data forced the size of the working matrix to be reduced to 10×128. Their rows were standardized in order to get a new matrix **Z**, and the correlation matrix **R** = **ZZ**′ (where **Z**′ represents the transpose of **Z**) was built (Kutzbach 1967). This symmetric, positive definite matrix was used as input for an unrotated principal components analysis (PCA) method (Richman 1986, and references therein). The outcome is 10 spatial patterns, named empirical orthogonal functions (EOFs), that are orthonormal to
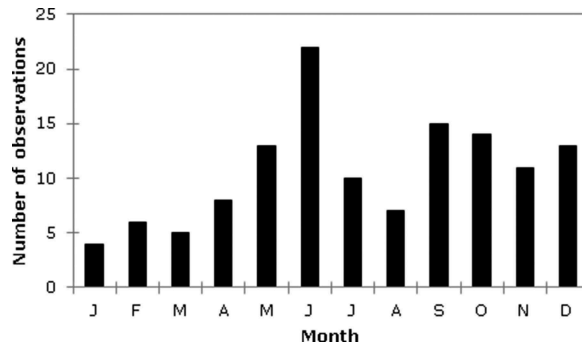
Figure 1. Number of cirrus observations used in this research.

each other. In addition, their associated expansion coefficients, so-called principal components (PCs), are uncorrelated in time. Results are presented in the next section.

3. Results

Table 1 shows the eigenvalues for each mode of variability and the represented variance along with the cumulative variance. The summation of all the eigenvalues equalling 10 is a consequence of **Z** having its rows standardized. According to Table 1, the first three modes account for just above 75% of the variance. Given that this percentage slightly exceeds the lower threshold in the subjective criterion $70\% \leq R^2_{\text{crit}} \leq 90\%$, which was suggested by Jolliffe (2002) in order to enclose the minimum represented variance R^2_{crit}, only these three modes are analysed. Rotation for these was not necessary because of the North et al. (1982) rule of thumb that relates the shift of any pair of eigenvectors with the spacing of the corresponding eigenvalues, including their shifts. The three EOFs are presented in Figure 2. Given that the 128 different cirrus observations were sparsely distributed throughout a five-year period between February 2002 and January 2007, a suitable way to analyse the time-evolving expansion coefficients is from a monthly standpoint.

Figure 3 shows the evolution of the first three, monthly-averaged PCs. The most representative mode (EOF$_1$) retains approximately 37% of the variance. The direct mode (i.e. positive values of PC$_1$) occurs between May and October (Figure 3). At this time, the upper and lower boundaries of the cirrus indicate that, although both of them

Table 1. Eigenvalues and represented variance for the 10 EOFs. Cumulative variance is also shown.

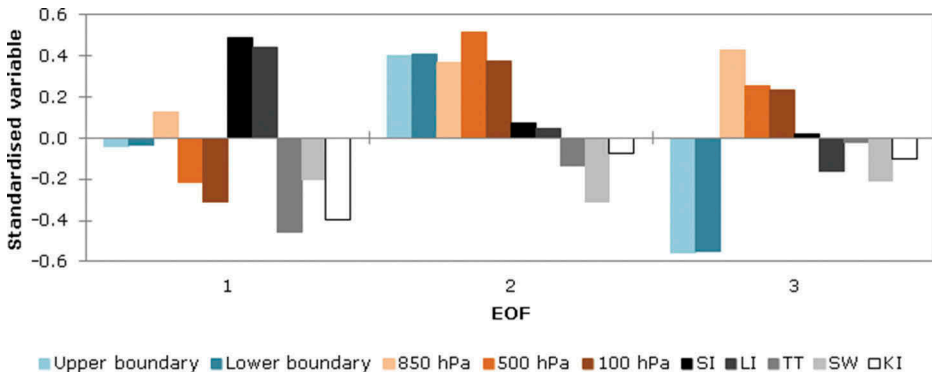| EOF	Eigenvalue	Represented variance (%)	Cumulative variance (%)
1	3.71	37.06	37.06
2	2.27	22.72	59.78
3	1.59	15.86	75.64
4	0.83	8.34	83.98
5	0.55	5.47	89.45
6	0.40	4.03	93.48
7	0.26	2.63	96.11
8	0.25	2.51	98.62
9	0.10	0.96	99.58
10	0.04	0.42	100.00

Figure 2. Anomaly patterns for the height of top and bottom of cirrus clouds, for heights of 850, 500, and 100 hPa, and for the Showalter index (SI), the Lifted index (LI), the total totals index (TT), the SWEAT index (SW), and the K-index (KI).
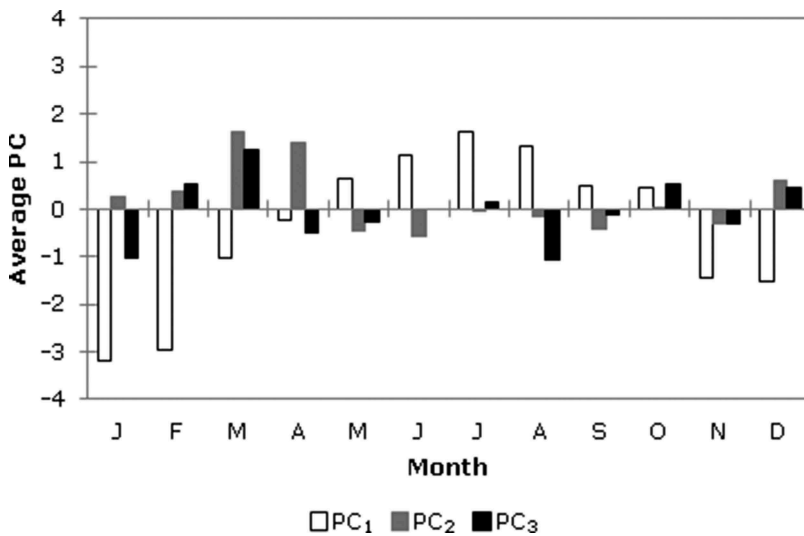

Figure 3. Monthly averages for the first three principal components (PCs).

experience a flat descent, this is larger for the top, so that the clouds tend to be slightly thinner than normal. The situation reverses for indirect modes (negative values of PC_1), between November and April (Figure 1), and cirrus is thicker than normal (Figure 2). Figure 2 shows that direct (indirect) modes are associated with ascent (descent) at the 850 hPa level, whereas 500 and 100 hPa behave the opposite way, with the latter level experiencing a larger deviation from its mean position.

Regarding the instability indices, a positive (negative) deviation from the mean for SI and LI shows a more stable (unstable) atmosphere for direct (indirect) modes. This instability is matched by the rest of the indices, for which anomalies are negative (positive) in direct (indirect) modes. Overall, the greater relative instability occurs during January and February, when water vapour concentrations are greatest (Kållberg et al. 2005, 38–39), and more stable conditions take place in July (Figure 1).

The second most representative structure (EOF_2) reflects both the top and bottom of the clouds being above (below) their mean values for direct (indirect) modes (Figure 2), in such a way that the cirrus is geometrically thinner (thicker) than in normal conditions. The largest deviations, of around 0.4σ, are even larger than in the EOF_1 case, but the absolute value of the standardized thickness is similar in both cases. The three mandatory levels for EOF_2 are in phase with each other and with the top and bottom of the cirrus, with 500 hPa showing the largest deviations($\approx 0.5\sigma$). Direct (indirect) modes occur between December and April (May and November), with maximum (minimum) values in March (June) (Figure 1). The greatest absolute values correspond to the direct mode, when the cirrus is displaced upwards from its mean position. Following the PC_2 time evolution, all instability indices are in line with a more (less) stable atmosphere, when compared to normal conditions, for direct (indirect) modes. Despite different PCs having no correlation with each other, monthly averages (Figure 3) show that PC_2 is generally in anti-phase to PC_1, meaning that one of the modes is stable when the other one is not.

EOF_3 direct modes correspond to both the top and bottom of the cirrus below their mean position (Figure 2). Anomalies are in the order of 0.6σ, being slightly greater at the cloud top thus making the clouds thinner. All three mandatory levels are above their mean positions, and 850 hPa exhibits the greatest departure, around 0.4σ. With the exception of SI, anomalies for the instability indices are negative. Overall, this makes the direct mode a stable one. Direct modes occur for positive PC_3 (i.e. in February–March, July, October, and December). The largest positive PC_3 values are in March (Figure 1). In contrast, indirect modes, which are unstable, occur in January, April–May, August–September, and November, with the largest negative values in August. Their associated modes correspond to all three mandatory levels being below their mean values, and the cirrus being slightly thicker with their top and bottom above their mean altitudes. By contrast with the opposing relationship between averaged values of PC_1 and PC_2 throughout the year, PC_3 seems to have no relationship with them at all.

According to the WMO, the thermal tropopause is defined 'as the lowest level at which the lapse rate decreases to 2ºC km^{-1} or less, provided that the average lapse rate between this level and all higher levels within 2 km does not exceed 2ºC km^{-1}' (WMO, 1992). The presence of multiple tropopause events (MTEs) is also considered in the definition, where their frequency shows a maximization in the extratropics (Yuchechen, Bischoff, and Canziani 2010). Considering double tropopause events (DTEs) only, Lakkis et al. (2011) found that three-quarters of cirrus clouds are located below the lower tropopause (LT) and that the remaining 25% are cross-tropopause cirrus (CTCs) with their top (bottom) above (below) LT.

The thermal tropopause at SAEZ was calculated following the WMO definition. The tropopause-finding algorithm used has the capability to detect up to five different tropopauses, but single tropopause events (STEs) and DTEs were by far the most frequent (Yuchechen, Bischoff, and Canziani 2010). Owing to missing tropopause data, the number of events available for cirrus observation was not 128 but 101, of which 44% corresponded with STEs. If single tropopauses (STs) are considered, none of the cirrus is entirely above it. CTCs account for ≈23% of the cases. Regarding DTEs, cirrus was found located below the upper tropopause (UT) in all cases, with just 12% crossing the LT level.

Correlation between height anomalies of these three different tropopauses and the first three PCs was carried out in order to establish how the structures shown in Figure 2 are linked to them. Two different correlation analyses are presented. The first, termed point-to-point (PTP) correlation, involves one of the original PCs and the height anomalies time series for each tropopause. These anomalies were calculated as departures from a 42-year-based (1973–2014) long-term mean. The other correlation will be referred to as Ave (for average) to distinguish it from the former, given that they use the monthly-averaged PCs, shown in Figure 3, plus the monthly mean values for tropopause height anomalies. The Pearson correlation coefficient, r between the first three PCs and height anomalies for the different tropopauses is shown in Table 2. It is worth noting that this coefficient strictly accounts for linear relationships between the pair of variables correlated so that the absence of significance does not necessarily mean the variables are unrelated in any way.

The PTP correlation between STE and PC_1 is significant and negative. This means that the pair in anti-phase (i.e. EOF_1 direct (indirect) modes – tied to cirrus descent (ascent) (Figure 2) – is partly linked to ST lowering (raising)). The Ave correlation is also significant but $|r|$ increases dramatically, reflecting a strengthening of the relationship between the described variables on a monthly basis. As to the ST/PC_2 and ST/PC_3 correlations, these are not significant for PTP. On the other hand, Ave shows significance and a positive value for r regarding ST/PC_2. Despite this result matching the one for ST/PC_1, in that a raising (lowering) in ST is related to an ascent (descent) of the cirrus with largest height anomalies for both the top and bottom in this case, the joint variability of the pair is less important than the ST/PC_1 one given that $|r|$ is smaller.

There is yet another similarity between ST/PC_1 and ST/PC_2 regarding the instability indices, since the EOF_1 and EOF_2 patterns are, as previously discussed, more stable (unstable) in direct (indirect) modes, and they are related to a raised (lowered) ST. For EOF_2, indirect modes also imply a descent of the three mandatory levels, with 500 hPa having the largest departure (cf. Figure 2). The indirect EOF_2 configuration is therefore in good agreement with the linkages between upper-level frontogenesis and tropopause lowering (Carlson 1998, 436–441), and stratospheric air intrusions into the troposphere and the destabilizing effects on the latter layer (Johnson 1986; Griffiths, Thorpe, and Browning 2000). In this respect, EOF_1 seems to be in contradiction because a tropopause lowering is associated with index anomalies that correspond to a more stable atmosphere. To the best of our knowledge, no research effort has been devoted to studying the connection between these two variables, either at the location studied here or

Table 2. Correlations between height anomalies of the different tropopauses and cirrus thickness anomalies with the first three PCs. PTP indicates point-to-point correlations, whereas Ave denotes that the monthly-averaged time series have been correlated (see text for further details). Values marked with an asterisk are significant to a 95% level of confidence.

	PC_1		PC_2		PC_3	
	PTP	Ave	PTP	Ave	PTP	Ave
Single tropopause (ST)	−0.53*	−0.94*	0.27	0.64*	0.01	0.22
Lower tropopause (LT)	−0.20	−0.86*	0.42*	0.65*	−0.16	0.20
Upper tropopause (UT)	−0.11	−0.68*	0.13	0.39	0.00	0.16
Cirrus thickness	−0.01	0.59*	−0.11	−0.44	0.10	0.32

elsewhere in the world. So, more research is required to shed light on this topic and to interpret these results.

Nevertheless, the vertical displacement for the cirrus in EOF_1 is in good agreement with the results found in Nahir et al. (2012), who reported that, on average, 20% of the cirrus clouds present over a tropical location in India are in a descending regime. Seeing that EOF_1 represents roughly 40% of the total variability (cf. Table 1), the annual cycle shown in Figure 3 leads to the conclusion that descending cirrus occurs 50% of the time (i.e., 20% of cases). Results here are limited to the way cirrus data were acquired, i.e. restricted to clear-sky days, with cirrus visible from the ground and absence of aerosols or pollutants (Lakkis, Lavorato, and Canziani 2009).

Also shown in Table 2 is the correlation between the first three PCs and cirrus thickness anomalies. Ave for PC_1 is the only significant correlation; its positive value means that, on a monthly basis, EOF_1 direct (indirect) modes are associated with thicker (thinner) cirrus. It is worth noting that this result cannot be estimated solely from the spatial and temporal behaviour of EOF_1 since, as pointed out before, direct modes reflect thinner clouds. Considering that the three Ave correlations between PC_1 and the different tropopauses are negative, and that between PC_1 and cirrus thickness is positive, it can also be concluded that thicker (thinner) cirrus is associated with tropopause descent (ascent), irrespective of the tropopause considered.

Regarding LT, Table 2 shows that the LT/PC_1 PTP correlation is not significant but that Ave is, with the value of r very close to that of ST/PC_1. This is most likely related to the fact that, on average, SAEZ LT gets closer to ST in the austral winter months (Bischoff, Canziani, and Yuchechen 2007) and the maximum number of cirrus observations in our data set occurs in June. Considering that the largest number of cirrus is located entirely below either the ST or the LT, the outcome also points to the accompanying vertical displacement of cirrus and these two tropopauses. The LT/PC_2 relationship is significant for both PTP and Ave, having the variables in phase in both cases, with a greater value for r in the latter. Again, this marks a direct connection between tropopause and cirrus height anomalies. There is no significance at LT/PC_3 for either PTP or Ave. If UT is considered, Table 2 shows that there are no PTP relationships with any PC. However, Ave shows the UT/PC_1 relationship is in line with both ST/PC_1 and LT/PC_1. This is once again in agreement with the findings of Bischoff, Canziani, and Yuchechen (2007) for SAEZ, because the UT annual evolution resembles that for both ST and LT. In the light of these results, the EOF_3 pattern cannot be related to fluctuations in tropopause height.

4. Summary and concluding remarks

The role played by cirrus clouds in the atmosphere is mainly related to the radiative budget, but their formation, presence, and persistence is associated with instability phenomena and convective processes. Atmospheric instability, addressed through instability indices, provides a real-time overview of atmospheric conditions. To address the relationship between cirrus clouds and atmospheric instability, this work is aimed at establishing the most representative patterns for the joint variability between the thickness of cirrus clouds, the geopotential height of the 850, 500, and 100 hPa mandatory levels, and five instability indices over Buenos Aires. Unrotated principal components analysis (PCA) was applied to obtain the joint variability modes between

height anomalies of the upper and lower boundaries of cirrus clouds and the three mandatory levels, and the anomalies of the instability indices. Only the first three structures were discussed given that they altogether account for approximately three-quarters of the total variance. Furthermore, the time series associated with each of these structures, termed principal components (PCs), were correlated with the time series for the height anomalies of different tropopauses in order to establish whether they are associated with fluctuations in the tropopause position.

The first most representative spatial structure, EOF_1, shows a direct (indirect) mode that sees the cirrus slightly below (above) its mean position, with 500 and 100 hPa exhibiting a similar behaviour and 850 hPa acting the opposite way. Above-normal stability (instability) is present in direct (indirect) modes for positive (negative) values of PC1. On a monthly basis, these occur in the austral winter (summer) months. Depending upon the sign of PC1, EOF_1 exhibits the largest stability or instability of the three EOFs discussed. Ave correlations between PC_1 and height anomalies of different tropopauses and between PC_1 and thickness anomalies of cirrus clouds showed that tropopause subsidence (rising) is connected with thicker and lower (thinner and higher) cirrus, regardless of the tropopause considered, a result that cannot be interpreted from the cirrus structure in EOF_1.

As to EOF_2, all three mandatory levels show positive (negative) height anomalies for direct (indirect) modes, with 500 hPa having the largest deviations, and an ascent (descent) of the cirrus amid mild stability (instability). PC_2 is mostly positive during summer and in early fall and negative the rest of the year. Ave correlations with different tropopauses indicate that indirect EOF_2 modes are in agreement with a relative destabilization of the troposphere. EOF_3 is characterized by stability that is similar to that of EOF_2, with direct (indirect) modes showing lowered (raised) cirrus and all three mandatory levels above (below) normal conditions. On a monthly average, PC_3 is best described as having a semi-annual evolution, with maxima in March and October and minima in January and August. No relationships with the vertical displacement of any tropopause can be inferred for EOF_3 from the correlations presented.

It is worth noting that, despite the number of observations of cirrus clouds included in the analysis (128 for the PCA and 101 for the tropopause correlations), our results permit the linking of atmospheric instability and the behaviour of three different mandatory levels to basic properties of such clouds over Buenos Aires. The main goal of the paper is to provide a characterization of the aforementioned topic, which is the first of its kind worldwide. It is important to point out that, even though the results are dependent on the interactions between cirrus clouds and local conditions (i.e. orography, general circulation systems, synoptic scale disturbances, mesoscale convective processes, etc.), the methodology can be easily replicated for other regions of the world having cirrus clouds observations that match radiosonde data for a given period. New cirrus observations are being acquired in order to complement the cirrus database used in this research and to provide further insight into the relationships described in this paper.

Acknowledgements

Disclosure statement

Funding

ORCID

Adrián E. Yuchechen ⓘ http://orcid.org/0000-0002-3823-2291

References

Bischoff, S. A., P. O. Canziani, and A. E. Yuchechen. 2007. "The Tropopause at Southern Extratropical Latitudes: Argentine Operational Rawinsonde Climatology." *International Journal of Climatology* 27: 189–209. doi:10.1002/joc.1385.

Carlson, T. N. 1998. *Mid-Latitude Weather Systems*. Boston, MA: American Meteorological Society.

Fujita, T. T. 1982. "Principle of Stereographic Height Computations and Their Application to Stratospheric Cirrus over Severe Thunderstorms." *Journal of the Meteorological Society of Japan* 60: 355–368.

Griffiths, M., A. J. Thorpe, and K. A. Browning. 2000. "Convective Destabilization by a Tropopause Fold Diagnosed Using Potential-Vorticity Inversion." *Quarterly Journal of the Royal Meteorological Society* 126: 125–144. doi:10.1002/qj.v126:562.

Holton, J. R., P. H. Haynes, M. E. McIntyre, A. R. Douglass, R. B. Rood, and L. Pfister. 1995. "Stratosphere-Troposphere Exchange." *Reviews of Geophysics* 33 (4): 403–439. doi:10.1029/95RG02097.

Howard, L. 1865. *Essay on the Modifications of Clouds*. Cambridge: Cambridge University Press. doi:10.1017/CBO9781139096966.

Jensen, E. J. L., T. V. Pfister, B. P. Lawson, B. Baker, Q. Mo, D. Baumgardner, E. M. Weinstock, J. B. Smith, E. J. Moyer, T. F. Hanisco, D. S. Sayres, J. M. St. Clair, M. J. Alexander, O. B. Toon, and J. A. Smith. 2008. "Formation of Large Ice Crystals near the Tropical Tropopause." *Atmospheric Chemistry and Physics* 8: 1621–1633. doi:10.5194/acp-8-1621-2008.

Johnson, R. H. 1986. "Short-Term Variations of the Tropopause Height over the Winter MONEX Area." *Journal of the Atmospheric Sciences* 43 (11): 1152–1163. doi:10.1175/1520-0469(1986)043<1152:STVOTT>2.0.CO;2.

Jolliffe, I. T. 2002. *Principal Components Analysis*. New York: Springer.

Kållberg, P., P. Berrisford, B. Hoskins, A. Simmons, S. Uppala, S. Lamy-Thépaut, and R. Hine. 2005. *ERA-40 Atlas*. ERA-40 Project Report Series No. 19. Reading: European Centre for Medium Range Weather Forecasts.

Kutzbach, J. E. 1967. "Empirical Eigenvectors of Sea-Level Pressure, Surface Temperature and Precipitation Complexes over North America." *Journal of Applied Meteorology* 6: 791–802. doi:10.1175/1520-0450(1967)006<0791:EEOSLP>2.0.CO;2.

Lakkis, S. G., M. Lavorato, P. Canziani, and H. Lacomi. 2015. "Lidar Observations of Cirrus Clouds in Buenos Aires." *Journal of Atmospheric and Solar-Terrestrial Physics* 130-131: 89–95. doi:10.1016/j.jastp.2015.05.020.

Lakkis, S. G., M. Lavorato, and P. O. Canziani. 2009. "Monitoring Cirrus Clouds with Lidar in the Southern Hemisphere: A Local Study over Buenos Aires. 1. Tropopause Heights." *Atmospheric Research* 92: 18–26. doi:10.1016/j.atmosres.2008.08.003.

Lakkis, S. G., M. Lavorato, P. O. Canziani, and H. Lacomi. 2011. "Cirrus Clouds and Multiple Tropopause Events over Buenos Aires." *Atmospheric and Climate Sciences* 2: 113–119. doi:10.4236/acs.2011.13013.

London, J. 1957. *A Study of the Atmospheric Heat Balance*. Final report. Contract AF 19(122)-165. New York: New York University.

Luce, H., N. Nishi, J.-L. Caccia, S. Fukao, M. K. Yamamoto, T. Mega, H. Hashiguchi, T. Tashiri, and M. Nakazato. 2012. "Kelvin-Helmholtz Billows Generated at a Cirrus Cloud Base within a Tropopause Fold/Upper-Level Frontal System." *Geophysical Research Letters* 39: L04807. doi:10.1029/2011GL050120.

Ludlam, F. H. 1951. "The Physics of Ice Clouds and Mixed Clouds." In *Compendium of Meteorology*, edited by T. F. Malone, 192–198. Boston, MA: American Meteorological Society.

Miller, R. C. 1972. *Notes on Analysis and Severe-Storm Forecasting Procedures of the Air Force Global Weather Central*. Tech. (200), AWS Technical Report. 200. Air Weather Service, United States Air Force. Offutt: Air Force Global Weather Central.

Nahir, A. K. M., K. Rajeev, M. K. Mishra, B. V. Thampi, and K. Parameswaran. 2012. "Multiyear Lidar Observations of the Descending Nature of Tropical Cirrus Clouds." *Journal of Geophysical Research* 117: D1821. doi:10.1029/2011JD017406.

North, G. R., T. L. Bell, R. F. Cahalan, and F. J. Moeng. 1982. "Sampling Errors in the Estimation of Empirical Orthogonal Functions." *Monthly Weather Review* 110: 699–706. doi:10.1175/1520-0493 (1982)110<0699:SEITEO>2.0.CO;2.

Petty, G. W. 2008. *A First Course in Atmospheric Thermodynamics*. Madison, WI: Sundog Publishing.

Reutter, P., and P. Spichtinger. 2013. *Geophysical Research Abstracts Vol. 15, (European Geosciences Union General Assembly* 2013): *Impact of cirrus clouds on tropopause structure and tracer distributions*. Vienna: European Geosciences Union.

Richman, M. B. 1986. "Rotation of Principal Components." *Journal of Climatology* 6: 293–335. doi:10.1002/joc.v6:3.

Sassen, K. 2002. "Cirrus Clouds: A Modern Perspective." In *Cirrus*, edited by D. K. Lynch, K. Sassen, D. O'C. Starr, and G. Stephens, 11–40. New York: Oxford University Press.

Sassen, K., and B. S. Cho. 1992. "Subvisual-Thin Cirrus Lidar Dataset for Satellite Verification and Climatological Research." *Journal of Applied Meteorology* 31: 1275–1285. doi:10.1175/1520-0450 (1992)031<1275:STCLDF>2.0.CO;2.

Sassen, K., Z. Wang, and D. Liu. 2009. "Cirrus Clouds and Deep Convection in the Tropics: Insights from CALIPSO and Cloudsat." *Journal of Geophysical Research* 114: D00H06. doi:10.1029/ 2009JD011916.

Stephens, G. 2002. "Cirrus, Climate, and Global Change." In *Cirrus*, edited by D. K. Lynch, K. Sassen, D. O'C. Starr, and G. Stephens, 433–448. New York: Oxford University Press.

Wada, E., H. Hashiguchi, M. K. Yamamoto, M. Teshiba, and S. Fukao. 2005. "Simultaneous Observations of Cirrus Clouds with a Millimeter-Wave Radar and the MU Radar." *Journal of Applied Meteorology* 44: 313–323. doi:10.1175/JAM2191.1.

Wang, P. K. 2004. "A Cloud Model Interpretation of Jumping Cirrus above Storm Top." *Geophysical Research Letters* 31: L18106. doi:10.1029/2004GL020787.

WMO (World Meteorological Organization). 1992. *International Meteorological Vocabulary*. WMO No. 182, Secretariat of the World Meteorological Organization. 2nd ed. 784 pp. Geneva: World Meteorological Organization.

Wylie, D. P., W. P. Menzel, H. M. Woolf, and K. I. Strabala. 1994. "Four Years of Global Cirrus Cloud Statistics Using HIRS." *Journal of Climate* 7 (12): 1972–1986. doi:10.1175/1520-0442(1994) 007<1972:FYOGCC>2.0.CO;2.

Yuchechen, A. E., S. A. Bischoff, and P. O. Canziani. 2010. "Latitudinal Height Couplings between Single Tropopause and 500 and 100 Hpa within the Southern Hemisphere." *International Journal of Climatology* 30: 492–508. doi:10.1002/joc.1914.